

Ceramics from Villa El Salvador, a late formative site from the Central Coast of Peru

Mercedes Delgado^a, Paula Olivera^b, Eduardo Montoya^b, Angel Bustamante^c

^a QALLTA, Centro de Investigación para la Preservación y Promoción del Patrimonio Cultural.
Jr. Luis Romero 1065, Lima, Perú

^b Lab. de Fluorescencia de Rayos X. Instituto Peruano de Energía Nuclear.
Apartado Postal 1687 Lima 41, Perú

^c Facultad de Ciencias Física, Universidad Nacional Mayor de San Marcos.
Apartado Postal Lima 14-0149. Lima, Perú

Abstract

We applied a multielemental analytical method for characterization of archaeological ceramics from Villa El Salvador. The ceramics were characterized using Instrumental Neutron Activation Analyses (INAA), Energy-Dispersive X-ray Fluorescence (EDXRF) and X-ray Diffraction (XRD) techniques. Whole vessels with no accurate provenience and Villa El Salvador ceramics sherds were analyzed. The EDXRF system can measure both the whole vessels and ceramics sherds. The results from the whole vessels were in good agreement with the results obtained from the ceramics sherds, with one exception. Thus, the comparison of the EDXRF spectra of the whole vessels with the data base of the Villa El Salvador sherd collection allows us the identification of distinctive groups of the site.

1 Introduction

Archaeological chronologies are based on the typological classification of the ceramics; multielemental analytical methods for characterization of ceramics and X-ray diffraction were used to identify the mineral composition of a group of samples.

The Villa El Salvador collection comes from funerary contexts; most are whole vessels. The ceramic corpus has been classified into groups on the basis of morphological and stylistic features [1]. The principal types of vessels are bottles, jars and ollas decorated with white painted designs executed on the unpainted surface or red slip paint on a zone of white paint. The determination of chemical characteristics of a group of whole vessels without accurate provenience was done by EDXRF non-destructive technique.

This study case was initiated as an inter-laboratory collaboration between the Archaeometry Laboratory of the University of Missouri-Columbia Research Reactor Center (MURR) and the Peruvian Institute of Nuclear Energy (IPEN), established in 1996.

The site is located in the lower Lurín valley on the central coast of Peru; Villa El Salvador is a district, south of Lima, ca. 1 km northwest of the archaeological area of Pachacamac, and 1 km north of El Panel, and 4 km southwest of

Tablada de Lurín. The Lomo de Corvina



Figure 1. Map of the central coast.

There were two survey projects at Villa El Salvador (Patterson, 1962 and Delgado, 1988)

and two excavations (Stohtert and Ravines 1975-76; and Delgado, 1990-91). The earliest excavation of the site was revealed the presence of a large cemetery with interments with cultural affiliation within the early phase of Lima Culture. The Villa El Salvador ceramic assemblage shows characteristics that cross-date to the end of the Formative Period (200 B.C. to 200 A.D.) and the early phases of Regional Development (Early Intermediate). (Fig. 2)

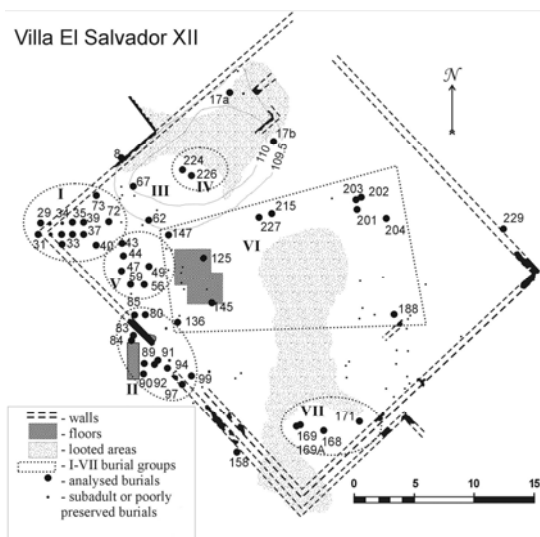


Figure 2. Map of the Site (VES XII).

There is still no complete ceramic sequence from the central coast that spans the time between the end of the Chavin influence and the beginning of the Lima style. At the central coast the replacement of the white-on-red styles by Lima style pottery is not clear, and we need to delineate this change.

2 Analytical methods

Trace-element analyses were conducted at the Department of Chemistry of the Peruvian Institute of Nuclear Energy (IPEN). Instrumental Neutron Activation Analyses (INAA) and Energy-Dispersive X-ray Fluorescence (EDXRF) were used to determine the chemical composition of the ceramic samples. X-ray diffraction (XRD) analyses were conducted at the Physics Science Faculty, Universidad Nacional Mayor de San Marcos.

2.1 Energy-Dispersive X-ray Fluorescence

The EDXRF system uses a Cd-109 source to activate the Ag K_α radiation of 22.101 KeV utilized to impinge to the sample, from which the energy of the x-ray emitted is detected by a

Si-Li detector and multichannel Analyzer PCA-II Nucleus for data acquisition.



Figure 3. EDXRF systems.

Samples were prepared and analyzed by two different procedures: conventional analyses use powder samples (Pellets, Φ 25-mm); and the alternate nondestructive methods involve placing the vessel across the X-ray specimen tray (Fig.3-5). All samples were irradiated for 4000 s.

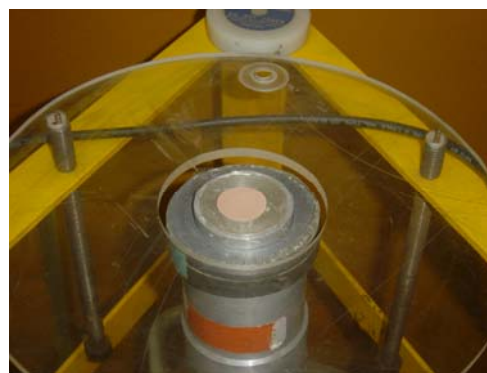


Figure 4. Powdered samples placed in the EDXRF.



Figure 5. Vessel placed across the X-ray tray

The spectra evaluation and peak fitting was made using the Quantitative X-ray Analysis System (QXAS-AXIL), IAEA Software. The calculation of the concentration was made using the Fundamental Parameters method, and the Ohio Red Clay was used as reference sample, (for results see Table 1).

2.2 Instrumental Neutron Activation Analyses

The IPEN has a 10 MW reactor (RP-10) type pool. All samples were irradiated at a nominal

neutron flux of $2 \times 10^{13} \text{ n cm}^{-2} \text{ s}^{-1}$; the pneumatic transfer system to control irradiation and decay times was used.

Data reduction of the gamma spectra was accomplished using DBGAMMA v 5.0 software. Quality control was assessed by periodical analysis of reference materials (Table 1).

Table 1. Analytical inter-comparison in Red Clay New Ohio sample.

Element	Ohio USA	INNA Brasil	INNA Perú	FRX Perú
Na (%)	0,144 ± 0,003	0,146 (0,143)	0,144	—————
K (%)	—————	—————	—————	4,01 ± 0,02
Sc (ppm)	17,8 ± 0,3	18 (19)	17,3 ± 0,9	—————
Ti (ppm)	—————	8065 (6900)	6220 ± 220	7678,2 ± 86
V (ppm)	—————	210 (197)	203 ± 15	—————
Cr (ppm)	90,1 ± 2,8	70 (95)	81 ± 3	< 88,79
Mn (ppm)	—————	230 (240)	253 ± 5	261,8 ± 15,8
Fe (%)	5,16 ± 0,09	5,6 (5,2)	4,9 ± 0,2	5,05 ± 0,02
Co (ppm)	20,6 ± 0,6	21 (23)	21,8 ± 1,4	19,6 ± 4,3
Ni (ppm)	—————	120	—————	—————
Cu (ppm)	—————	—————	—————	27 ± 5
Zn (ppm)	106 ± 4	86	92 ± 8	109,8 ± 10
Ga (ppm)	—————	28	16,7 ± 0,9	27,7 ± 5,1
As (ppm)	14,1 ± 0,6	14	14,6 ± 1,3	16,5 ± 3,9
Rb (ppm)	200 ± 13	180	162 ± 8	190 ± 13,5
Sr (ppm)	—————	57	—————	69,4 ± 8,1
Y (ppm)	—————	—————	—————	112,7 ± 10,4
Zr (ppm)	—————	—————	—————	305,3 ± 17,1
Nb (ppm)	—————	—————	—————	24,8 ± 4,8
Mo (ppm)	35	—————	—————	—————
Sb (ppm)	1,48 ± 0,12	—————	1,21 ± 0,05	—————
Cs (ppm)	10,1 ± 0,3	9 (9)	10,3	—————
Ba (ppm)	689 ± 56	—————	610	—————
La (ppm)	54,5 ± 1	47 (48)	46,2 ± 0,7	—————
Ce (ppm)	106 ± 2	110 (106)	117 ± 4	109,5 ± 10
Nd (ppm)	43,7 ± 7	—————	55,6	—————
Sm (ppm)	8,87 ± 0,23	8,5 (9)	9,8 ± 0,46	—————
Eu (ppm)	1,46 ± 0,04	4 (2)	1,7 ± 0,05	—————
Dy (ppm)	—————	7	—————	7,5 ± 2,6
Pb (ppm)	—————	25	—————	9,9 ± 3
Th (ppm)	15,3 ± 0,4	18	15,0 ± 0,6	13,8 ± 3,6
U (ppm)	2,5 ± 0,5	2,5	2,88 ± 0,02	< 4,16

2.3 X ray Diffraction

XRD allow us to identify the mineralogical phases present in the ceramic samples [2]. The XRD measurements were done at the X-ray diffraction Laboratory of the Physics

ScienceFaculty, Universidad Nacional Mayor de San Marcos. The XRD equipment is a Rigaku, Miniflex model, system, equipped with Cu-K α ; radiation (30 kV, 15 mA) with monochromator and a goniometer in a vertical arrangement (see Fig. 6). The samples were prepared in powder

form and the 2-theta scanning range, step interval and time per step were selected at the operator's criteria. The minimum angle for the 2-theta scan was set at 5°. To identify the mineralogical phases the Hanawelt method was used, it consists of locating the reflections of greater intensity in each mineralogical phase. The mineral phases were identifying using the PCPDFWIN software from JCPDS- International Center for Diffraction Data.



Figure 6. DRX equipment.

3 Sample

Two shreds from different parts of the vessels, representing the different types of vessel shapes and paste were analyzed. The samples were taken from the same part of the vessel. We had the problem that the associated fragments to funeral contexts did not represent the totality of definite types in our classification. With comparative purpose they were analyzed a small group of entire vessels. The groups of the powdered samples include ollas, bottles and jars.

Preliminary analysis of the ware characteristics, the kind and size of the inclusions in the clays, colors and stylistic features are made. We define two types of wares, brown and orange.

The brown ware was done from a coarse sand, feldspars, stone, salts, and silica and quartz particles. Whereas the orange ware was done from fine sand, mica, feldspars, salts, silica and quartz particles.

The differences in ware characteristics are defined by the kind of inclusions and their sizes as by the colors of the finished pottery vessels.

3.1 Sample preparation

INAA / XRF

Powder was removed from the surface of the sample using a motorized hand drill and special high-purity tungsten carbide bits. The sherd was then washed, dried and pulverized in an agate mortar and pestle. The pulverized samples were transferred to glass vials and dried for 24 h at 105 °C. The mass of the samples were approximately 250 mg, and put into polyethylene vials and sealed for INAA.

Table 2. Ceramic samples (vessel types).

Sample	Site	Provenance	Type	Description
1	VES 12	N-22	2B2a	Ovoid jar
2	VES 12	C.F. 202	2B2a	Ovoid jar
3	VES 12	DIII1	2B2a	Ovoid jar
4	VES 12	C.F. 33	2B1a	Semiglobular jar
5	VES 12	C.F. 194	2B1a	Semiglobular jar
6	VES 12	C.F. 177	2B6	Globular jar
7	VES 12	C.F. 206	2B6	Globular jar
8	VES 12	C.F. 220	2B6	Globular jar
9	VES 12	C.F. 218	2B6	Globular jar
10	VES 12	Z13	2A5	Semiglobular small jar, incised handle
11	VES 12	C.F. 229	1B2	Globular olla
12	VES 12	C.F. 179	1B2	Globular olla
13	VES 12	C.F. 200	1B1a	Semiglobular olla
14	VES 12	DIII2	IB1b	Semiglobular squat olla
15	VES 12	IV-R19A	1A1	Semiglobular olla, painted designs
16	VES 12	X17B1	1A2	Semiglobular olla, with modeled lugs
17	VES 12	DIII3	1B1c	Semiglobular olla, modeled handle
18	VES 12	C.F. 33	IB2a	Globular olla, convex base
19	VES 12	CAT3	IB3	Lenticular shape Olla
20	VES 12	C.F. 163	3B1	Double-spout-and-bridge bottle
21	VES 12	C.F. 16	3C1	Ornitomorphic bottle
22	VES 12	DIII4	3C1	Ornitomorphic bottle
23	VES 12	DIII5	3C1	Ornitomorphic bottle
24	VES 12	C.F. 30	I.1	Antara fragment
25	VES 12	M16	I.2	Antara fragment

For the analysis of the vessels was chosen two or three points of irradiation, being careful of including homogeneous and sufficiently flat surface. Before the measurement the area was cleaned removing the superficial layer. The measurement area was a circle of around 2 – 3 cm diameter [3].

XRD

The surface of each sample was removed using a motorized hand drill and special high-purity tungsten carbide bits. Samples were grinding in

an agate mortar and pestle, taking care to get an uniform grain size. The powdered sample was placed in a 3 cm diameter holder and pressed to obtain a flat surface.

The 2-theta scan range was 5 and 65 degrees with a step interval of 0.04 degrees, with a counting time of 2 s by step.

Table 3. Irradiation time of whole vessels (FRX)

Sample	Identification #	Irradiation Point	Irradiation Time (s)
491	(VES 006/86) (Shaman/mas cara)	Base, left foot (491 A)	5000
		Base, right foot (493 B)	5000
		Body, right side(491 C)	5000
492	(VES 016/86) (Viejo Shaman)	Base, right foot (492 A)	5000
		Base, left foot (492 B)	5000
		Body, lower part (492 C)	5000
493	(VES 014/86) (Felino)	Body, lower part (493 A)	4000
		Body, left side (493 B)	4000
		Body, lower part (494 A)	4000
494	(VES 017/86) (Mono)	Body, right side(494 B)	5000
		Base (495 A)	5000
495	(VES 023/86) (Ave sobre cactus)	Body left side (495 B)	5000

4 Results

All samples were submitted to both types of analysis, INAA and EDXRF [4]. The main concentrations of elements allow us determine groups of samples. The results of the analysis indicate presence of two differentiate groups of vessels.

The group of samples defines the cluster 1 and 2 obtained by EDXRF, these are based on the relation between the main components Fe and Sr. In Figure N° 7 we show the group obtained from the powdered samples, Figure N° 8 includes the data obtained from the whole vessels.

Table 3a and 3b give us the chemical composition of the samples obtained by XRF. Table 4 gives us the chemical composition of the

samples obtained by instrumental neutron

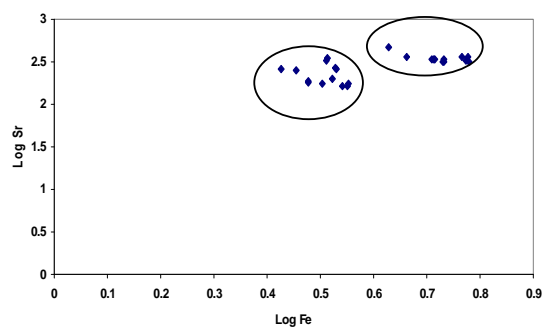


Figure 7. EDRXF composition analysis of powdered samples.

activation analysis.

The results obtained indicate that both types of analysis permit to obtain results of the chemical composition of the ceramics samples. Cluster analysis shows similarities in the chemical composition.

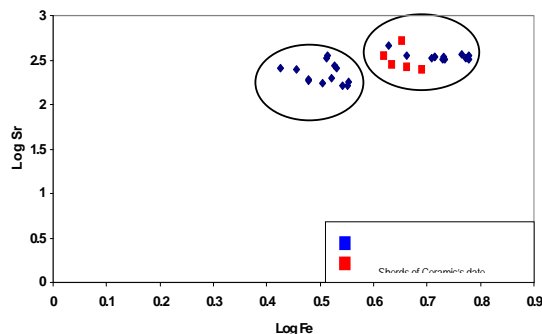


Figure 8. EDRXF composition analysis including whole vessels.

Although X-ray fluorescence analysis from the powdered samples gives us only concentrations of 7 elements, neutron activation provides us 28 elements, the similarity of the concentrations in the elements show that we can correlate the data of both techniques. (Fig. N° 9)

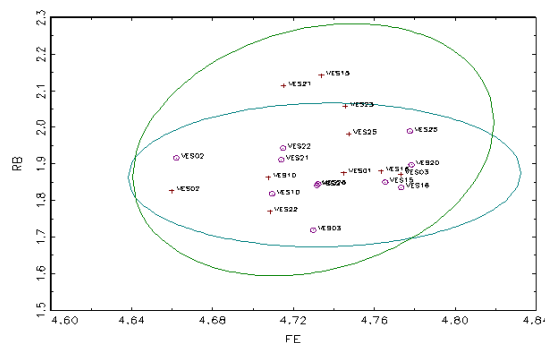


Figure 9. NAA and EDRXF composition analysis of powdered samples.

Table 4a. Elemental composition of powdered samples (EDXRF).

Sample	Ti (%)	Fe (%)	Rb (ppm)	Sr (ppm)	Y (ppm)	Zr (ppm)	Nb (ppm)
1	0.435	5.39	69.326	342.217	60.324	199.603	6.995
2	0.424	4.592	82.5	355.307	61.152	247.274	6.997
3	0.459	5.367	52.318	320.549	57.1	251.1	5.27
4	0.325	2.853	77.812	251.442	39.583	249.135	5.567
5	0.392	3.325	67.207	200.396	41.757	253.772	5.922
6	0.378	3.37	74.289	270.573	55.732	255.909	6.436
7	0.379	3.569	83.446	176.718	44.724	262.996	7.245
8	0.359	3.196	79.484	173.045	43.224	255.468	5.47
9	0.316	3.25	114.763	331.673	49.88	195.303	5.604
10	0.528	5.121	65.738	335.338	54.732	207.153	6.475
11	0.389	3.391	67.883	258.245	68.567	255.513	7.171
12	0.312	3.48	74.595	165.038	40.423	257.923	6.042
13	0.382	3.557	76.915	165.294	43.864	250.843	5.482
14	0.341	3.007	79.431	188.687	40.246	286.981	6.289
15	0.61	5.827	70.806	362.238	63.021	259.611	8.517
16	0.42	5.934	68.501	327.85	54.84	286.203	6.186
17	0.293	4.256	99.209	462.583	48.384	171.599	3.799
18	0.349	3.267	112.397	354.311	55.124	238.7	8.837
19	0.25	3.001	64.107	183.202	44.604	210.371	4.974
20	0.457	6.003	79.011	318.62	59.422	210.371	4.974
21	0.469	5.176	81.623	342.298	63.013	355.562	9.915
22	0.386	5.187	87.777	341.723	50.695	200.515	6.515
23	0.397	5.398	69.973	318.895	46.03	224.536	7.762
24	0.57	2.665	78.63	258.669	39.845	381.042	13.946
25	0.556	5.992	97.53	357.557	56.1	230.062	10.16

Table 4b. Elemental composition of ceramic vessels (EDXRF).

Sample	VES 006/86 (Shaman/mascara)			VES 016/86 (Viejo Shaman)			VES 014/8 (Felino)		VES 017/86 (Mono)		VES 023/86 (Ave sobre cactus)	
	Point A	Point B	Point C	Point A	Point B	Point C	Point A	Point B	Point A	Point B	Point A	Point B
K	23353	34905	18566	23260	27160	27887	13477	21222	15455	24172	9822	17743
Ca	15575	17360	13467	13804	14108	18929	14429	18358	15249	19106	115038	17259
Ti	3017	2982	2869	3044	3624	3712	3879	3521	3433	4502	< 1800	2935
Mn	663	654	667	581	554	719	572	702	506	527	111	833
Fe	35829	40014	41593	42605	42019	52395	45766	51572	38143	47977	5977	27919
Co	17	20	25	20	23	31	25	26	18	24	< 2	15
Cu	< 35	97	70	< 35	< 35	49	60	41	< 35	44	< 35	< 35
Zn	94	151	105	91	82	91	56	77	85	95	< 16	73
As	< 35	< 35	< 35	73	68	< 35	43	< 35	< 35	< 35	< 35	< 35
Br	< 6	< 6	< 6	< 6	< 6	< 6	< 6	< 6	< 6	< 6	90	< 6
Rb	64	75	67	70	71	64	46	59	57	73	< 7	84
Sr	336	360	358	261	259	296	230	263	265	311	727	310
Sb	< 310	< 310	< 310	< 310	< 310	< 310	< 310	< 310	< 310	< 310	727	< 310
Ba	< 525	< 525	< 525	< 525	< 525	< 525	< 525	< 525	< 525	< 525	1057	< 525
Pb	34	39	32	14	26	55	< 10	19	27	33	15000	134

The XRD patterns are shown in Fig. 10 and Fig. 11. Feldspars are clearly visible in the pattern, this reveals the presence of albite ($\text{NaAlSi}_3\text{O}_8$) and quartz (SiO_2) in the sample VES018 (double-spout and bridge bottle); the other sample, VES029 (jar), show the presence of both minerals and also microcline.

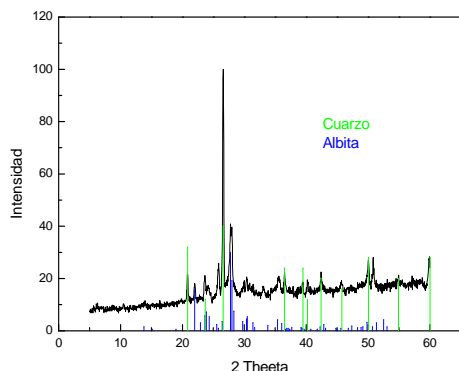


Figure 10. XRD pattern of the sample VES 018.

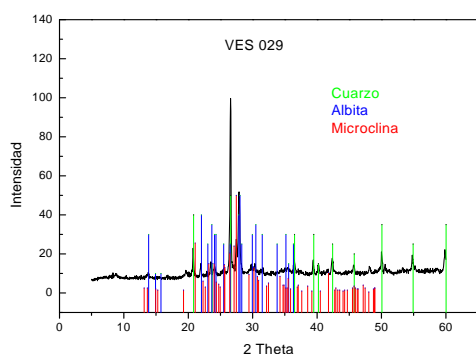


Figure 11. XRD pattern of the sample VES 029.

5 Conclusions

The application of a non-destructive energy-dispersive X ray fluorescence technique has increased the analytical potential for the study of ceramics whole vessels.

This study demonstrates that non-destructive trace element analyses on ceramics vessels and the conventional analysis can produce semi

quantitative data useful to correlate chemical characterization of both types of method [5].

We propose that the data from neutron activation analysis can be correlated with those obtained by x-ray fluorescence.

Comparison of data of both analyses allows choose the type of analysis that be better to our possibilities. Not always we include the possibility to carry out the analysis by neutron activation, by its cost and the time required, the analysis by XRF is considered like a valid alternative.

X- ray diffraction was used to complement the results from the chemical characterization, analysis of more samples could be correlate with the archaeology typology.

6 Acknowledgements

This work was supported by the Peruvian Institute of Nuclear Energy and the Universidad Nacional Mayor de San Marcos.

7 References

- [1] Delgado M. Análisis de materiales del sitio de Villa El Salvador. Unpublished report presented to the Instituto Nacional de Cultura, 2000.
- [2] Brindley GW, Brown G. Crystal structures of Clay Minerals and their X-Ray Identification. Mineralogical Society Eds; 1984.
- [3] Druc I. Caractérisation de céramiques archéologiques andines par fluorescence de rayons X. Journal de Physique IV. 2000 ; 10: 323-331.
- [4] Garcia Heras M. Analysis of archaeological ceramic by TXRF and contrasted with NAA. Journal of Archaeological Science. 1997; 24: 1003-1014.
- [5] Padilla Alvarez R, Van Espen PJM, Plá RR, Montoya Rossi E, Arrazcaeta Delgado R, Godo Torres P, Celaya González M. Compositional classification of archaeological pottery based on NAA and EPXMA. IAEA Report. 2001.